

# Growth Inhibition of Sulfate-Reducing Bacteria during Gas and Oil Production Using Novel Schiff Base Diquaternary Biocides: Synthesis, Antimicrobial, and Toxicological Assessment

Nabel A. Negm,\* Amal A. Altalhi, Nermin E. Saleh Mohamed, Maram T. H. A. Kana, and Eslam A. Mohamed\*



Cite This: *ACS Omega* 2022, 7, 40098–40108



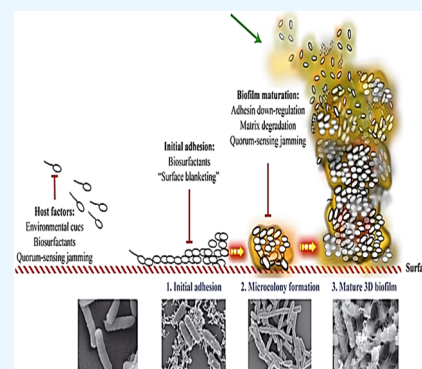
Read Online

ACCESS |

Metrics & More

Article Recommendations

**ABSTRACT:** Upstream crude oil production equipment is always exposed to destruction damagingly which is caused by sulfate-reducing bacterium (SRB) activities that produce  $H_2S$  gas, which leads to increased metal corrosion (bio-fouling) rates and inflicts effective infrastructure damage. Hence, oil and gas reservoirs must be injected with biocides and inhibitors which still offer the foremost protection against harmful microbial activity. However, because of the economic and environmental risks associated with biocides, the oil and gas sectors improve better methods for their usage. This work describes the synthesis and evaluation of the biological activities as the cytotoxicity and antimicrobial properties of a series of diquaternary cationic biocides that were studied during the inhibition of microbial biofilms. The prepared diquaternary compound was synthesized by coupling vanillin and 4-aminoantipyrine to achieve the corresponding Schiff base, followed by a quaternization reaction using 1,6-bromohexane, 1,8-bromooctane, and 1,12-bromododecane. The increase of their alkyl chain length from 6 to 12 methylene groups increased the obtained antimicrobial activity and cytotoxicity. Antimicrobial efficacies of Q1–3 against various biofilm-forming microorganisms, including bacteria and fungi, were examined utilizing the diameter of inhibition zone procedures. The results revealed that cytotoxic efficacies of Q1–3 were significantly associated mainly with maximum surface excess and interfacial characteristics. The cytotoxic efficiencies of Q1–3 biocides demonstrated promising results due to their comparatively higher efficacies against SRB. Q3 exhibited the highest cytotoxic biocide against the gram +ve, gram –ve, and SRB species according to the inhibition zone diameter test. The toxicity of the studied microorganisms depended on the nature and type of the target microorganism and the hydrophobicity of the biocide molecules. Cytotoxicity assessment and antimicrobial activity displayed increased activity by the increase in their alkyl chain length.



## 1. INTRODUCTION

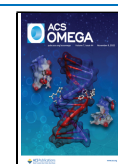
Autochthonous microorganisms flourish in anoxic environments under high pressure, temperature, and salinity in crude oil and gas reservoirs.<sup>1</sup> Oil reservoir bacterial species are known as a global range of bacteria and archaea which have effectively acclimated to such physicochemical circumstances.<sup>2</sup> The antimicrobial activity in such habitats is essential for the oil industry because of the consequences that some of these organisms may have on extracting operations such as producing hydrogen sulfide (souring), metal corrosion, and pipeline plugging.<sup>3,4</sup> Aerobic and anaerobic bacterial growth has damaged the majority of the worldwide petroleum produced,<sup>5</sup> lowering its value and quality. The equilibrium between attraction and repulsion interactions of bacteria and solid interfaces has been termed bacterial adsorption. The nature of the bacterial strain, surfaces, concentration of nutrients, and the contact of bacterial cells with their community influence the type of the occurred interaction. The adhering property of bacteria is linked to flagella,

lipopolysaccharides, and proteins in their outer membrane.<sup>6</sup> Long-range forces like steric and electrostatic interactions, in addition to short-range forces including van der Waal forces, acid–base, hydrogen bonding, and bio-specific interactions, drive the bacterial adsorption.<sup>7</sup> Bacteria can be found in two communities: planktonic (freely spread and living in bulk solution) or sessile (attached to a surface or contained inside the boundaries of a biofilm). Planktons are water-living organisms. Its name is derived from the Greek word “planktos”, which means “drifter”. Planktons come in a variety of sizes and forms. Planktons can be classified under three

Received: July 30, 2022

Accepted: October 20, 2022

Published: October 28, 2022



classes: plants, animals, and bacteria (phytoplanktons, zooplanktons, and bacterioplanktons).<sup>8</sup>

Animal planktons (zooplanktons) are ranged from protozoans and rotifers as small microscopic organisms to macroplanktons of larger size, including fish larvae, shrimp, and jellyfish. Macroplanktons are not like phytoplanktons, light-independent for nutrition. Macroplanktons voyage to the water surface to feed on phytoplanktons or small zooplanktons during the night and sink at daylight. On the other hand, light and nutrients are required for phytoplanktons to feed. The high temperatures stimulate the population growth of phytoplanktons, especially in the presence of increased nutrient concentration. This dense blossoming turns the clear color of seawater into opaque. The dense layer and populations of phytoplanktons have an inverse influence on the environment “aquatic system” due to the blocking of the sunlight to penetrate the deep layers of the aquatic system and the consumption of the dissolved oxygen in this system. The death and decomposition of phytoplanktons release some polluting products and gases.

A biofilm<sup>9</sup> is a microbial-produced sessile community that adheres to an interface or each other. Simply, bacterial cells adhere to the surfaces via extracellular polymeric gelatinous nucleic acids, polysaccharides, and protein compounds.<sup>10</sup> The adsorption displays an improved phenotype concerning growing progress and gene coding compared to their free-floating (so-called planktonic form) counterparts.<sup>11</sup>

A biofilm is an organized population of bacteria that live inside a self-created matrix of polymeric substances that adhere to a variety of interfaces.<sup>12</sup> These microbial communities have been discovered in practically every habitation, on both biotic and abiotic interfaces, as floated or submerged.<sup>13</sup> Biofilms are bacterial colonies that are either homogeneous or heterogeneous and are implanted in an extracellular polymeric matrix (EPS). Polysaccharides are the majority of EPS, in addition to some biomolecules including nucleic acids, lipids, and proteins.<sup>14</sup> Biofilms are hydrogels with viscoelastic characters, allowing them to resist mechanical stress.<sup>15</sup> The effectively trapped nutrients and water (due to the hydrogen bonds) in the EPS matrix with the polysaccharides are available to the bacteria.<sup>16</sup>

The formation of biofilms is a complex process, and their formation comprises several routes which are as follows: development of surface conditioning films; adjoining the microorganisms to the surface; adhering of microbe cells on the conditioned surface in the irreversible and reversible process; progression of the adhered microbe cells via division to form colonies in the form of biofilms, including phenotype alterations either with or without gene code modification; and separation of the formed biofilms in the patch form of scattered cells.<sup>17</sup>

**1.1. Mechanism of Bacterial Adsorption.** Motile and floated bacterial cells in the fluids can be found in the bulk, where cells are not subjective to the surface conditions, and sub-surface, where the hydrodynamic movement of the surface can impact the bacterial cells.<sup>18</sup> Two reported physicochemical approaches illustrated the adsorption and interaction of biofilms on the surfaces. The first is the thermodynamic approach which considered the surface free energies of the interacting surfaces, with no consideration for the electrostatic interactions. The second approach is the Derjaguin–Landau–Verwey–Overbeek (DLVO) approach, which considers the decay of Lifshitz–van der Waals and the electrostatic

interactions by increasing the distances between the surfaces. The two approaches have described the benefits of a typical bacterial colony’s attachment to the surfaces but were unsuccessful in the generalization of all aspects of the bacterial strain’s adsorption description.<sup>19</sup>

The thermodynamic approach<sup>20</sup> considers the different modes of interactions (attraction and repulsion), e.g., van der Waal, electrostatic, and dipole moment in thermodynamic numerical expressions of surface free energies of bacterial, substratum, and medium surfaces to estimate the Gibbs energy of bacterial biofilm adsorption. Negative values of Gibb’s adsorption energy revealed the spontaneous adsorption of bacterial biofilms onto surfaces. According to the thermodynamic standpoint, bacterial adsorption can be accounted for through three theories, which are polar-dispersion components, the Neumann equation, and Lewis acid–base theory.<sup>21</sup>

The polar-dispersion method pointed to the bacterial adsorption onto surfaces in the lack of any specific interfacial interactions. However, this postulation strongly conflicts with the intermolecular interactions of complex phases. Neumann’s theory neglects the influence of the molecular characteristics of the medium or surface on the adsorption tendencies of the bacterial biofilms and considers only the contact angle between the bacterial cell surface and the substrate. The Lewis acid–base (electron donor–acceptor) treatment neglects the dipole impact on intermolecular forces,<sup>22</sup> and hydrogen bonding is the predominant factor accountable for the adsorption process. The thermodynamic approach can be applied for energetically isolated systems, which do not occur in real bacterial biofilm media.

DLVO theory confirmed that the adsorption process is distance-dependent. Furthermore, it succeeded in explaining the increasing tendency of bacterial adsorption by increasing the hydrophobicity of substrates or bacterial membranes. However, DLVO could not explain the interaction of a highly hydrated surface (as in the case of bacterial cell membranes), which requires displacing the water molecules (energetically unfavorable) from the adjacent surfaces before adsorption.

Extended DLVO theory<sup>23</sup> considered the hydrophilic–hydrophobic interaction during the bacterial cells’ adsorption; hence, the overall energy of adsorption is expressed (eq. 1):

$$\Delta G^{\text{adh}} = DG^{\text{AB}} + DG^{\text{vdW}} + DG^{\text{dl}} \quad (1)$$

where  $DG^{\text{vdW}}$ ,  $DG^{\text{dl}}$ , and  $DG^{\text{AB}}$  represent acid–base, van der Waals, and double-layer interactions, respectively.

DLVO theory can describe the overall interaction between the surface and the adsorbed bacterial cells throughout the attractive interaction (van der Waal) and the repulsive interaction (double layers and Coulomb interactions). Additionally, it could not describe several key points during the bacterial cells’ adsorption onto the surfaces. These drawbacks of explanation can be pointed out as follows: (i) the low bacterial adsorption onto negatively charged interfaces, (ii) the low or weak adsorption in substantially concentrated electrolytes, (iii) the numerous molecular interactions, when components of the bacterial membrane are contacted by the backbone of the interface and conditioning film, and (iv) the bacterial cell–interface distance which influences the interaction types.

Extended DLVO theory considered the distance parameter in the calculation of the adsorption energy, in addition to the attraction between hydrophobic surfaces and repulsion between similarly charged interfaces in terms of double layer

and acid–base interactions. The complicated systems of bacterial cell–polymer surface composition (including the variation of the polymer composition due to the change in the surrounding conditions, contaminants, or time) require more experimental observations during bacterial adsorption.

Bacterial cells can be classified into motile (having flagella, fimbriae, and pili) and nonmotile without any type of flagellum on their surface. Flagella help the bacterial cells to adsorb at the interfaces at low, moderate, and high flow solutions, while in the absence of flagella, bacterial cells adsorb at low or moderate flow solutions. In fast flow solutions or surroundings, the nonmotile bacterial cells stay suspended in the medium<sup>24</sup> (Figure 1). The flagella and their number on the bacterial cells

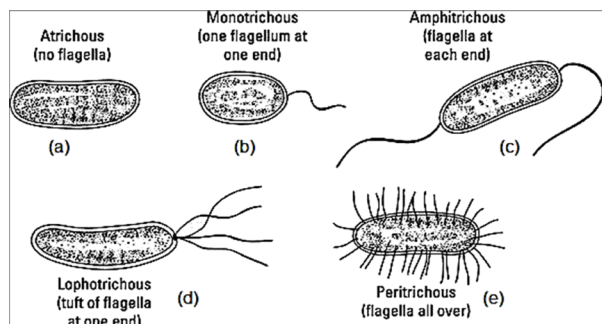


**Figure 1.** Bacterial cells: (a) without flagella and (b–e) with different types of flagella.

play an important role in their tendencies toward adsorption onto the interfaces. *E. coli* strain (motile by several flagella) has upsurged population in its inactive state (spores) with fast deposition onto the interfaces,<sup>25</sup> while the opposite occurs in the case of *V. parahaemolyticus* bacterial strain (motile with one flagellum).<sup>26</sup>

The adsorption of bacterial cells onto the interfaces occurred initially by the contact between the cells and the interface. Then, two main steps occurred to accomplish the adsorption of the cells onto the surface: the first is the primary attachment, and the second is the irreversible adsorption of the bacterial cells. The first step occurred fast (within 1–5 min) and is characterized by reversibility,<sup>27</sup> which occurred through van der Waals and positive–negative interactions between the negatively charged bacterial cell membranes<sup>28</sup> and the positively charged interface, while the second step is slow “within several hours” resulting in a consolidated irreversible adsorbed bacterial film on the surface through several interactions. These interactions are dehydration of the interface, conformation changes of the outer surface molecules, and relocation of the bacterial cells on the interface to reach the maximum anchoring.<sup>29</sup> Quorum sensing in *E. coli* causes an increase in the negative charge on cell surfaces, which may facilitate the interaction of bacteria with surfaces during the initial stages of biofilm formation.<sup>30</sup> Tightening the attachment of the bacterial cells on the surfaces occurred via chemical attachment with the aid of some chemical species on the cellular membrane. For example, *P. aeruginosa* is irreversibly attached to the surface by SadB cytoplasmic protein,<sup>31</sup> while *E. coli* bacterial cells are attached to the surface by lipopolysaccharide and pili.<sup>32</sup> *P. fluorescens* use ABC transporter protein<sup>33</sup> in their flagella and secrete EPS extracellular polymeric compounds to attach the biofilm on the surfaces. The attachment of bacteria occurred preferentially depending

on the nature of the surface; *S. mutans* attached tightly to the teeth surface and did not attach to the mouth’s inner skin. Motility promoters (organelles) in the bacterial cells are terminated by specific types of proteins which facilitate the adsorption and attachment of the bacterial cells on the surface. Organelles can be divided into pili (fimbriae), curli, and flagella (Figure 2).

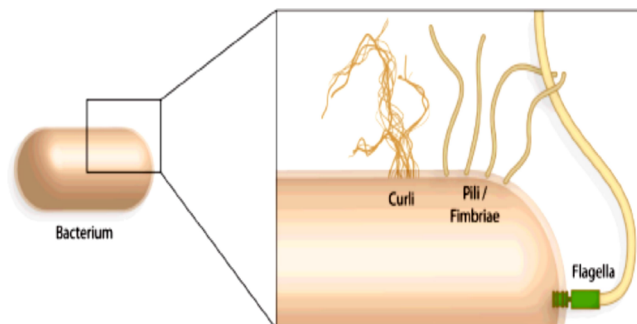


**Figure 2.** Bacterial surface has several organelles that facilitate interactions with substrates, including curli fibers, pili, and flagella.

The reversibility or irreversibility of the bacterial attachment to surfaces depends on the mode of that attachment and the bacterial strains forming the biofilm or colonization. *E. coli* attach to surfaces in a reversible process on the terminal mannose residues presented in the outer cellular glycoproteins throughout FimH in their pilus.<sup>34</sup> The binding of FimH depends on the shear stress threshold, which undergoes a reversible or irreversible process during bacterial biofilms or colony formation.<sup>35</sup> Specific adsorption of the bacterial biofilm on the surfaces was reported for *F. johnsoniae* which has SprB as a specific attachment promoter on the agar surface. A biological study was made on the SprB genome of *F. johnsoniae* to enhance its attachment on other surfaces, like glass.<sup>36</sup>

Bacterial attachment to surfaces is disagreeable in the environment, including medical implantations,<sup>37</sup> water refinement systems, marines, and many other industrial processes. Commonly, the biofouling of marine equipment originates from bacterial cell attachment before they develop into larger organisms, even in the presence of antifouling protective coatings.<sup>38</sup> Thermodynamics has a key role in controlling the attachment of bacteria to surfaces. The ability of bacterial attachment can be observed from their tendencies toward diverse material surfaces, including organic polymers, fluorinated surfaces such as polytetrafluoroethylene, aluminum, glass, and stainless steel.<sup>39</sup> It was reported that the surface energy of bacteria is smaller than the surface energy of the aquatic system where mostly the cells are presented, which explains the preferential tendencies of bacterial cells toward attachment to the hydrophobic surfaces. The challenge in the prevention of biofilm formation on surfaces is the hindrance of conditioning layer deposition. Regarding these challenges, the surface-resistance bacterial attachment is an excellent solution for the point. Several approaches were described regarding the reduction of bacterial biofilm attachment, including modifying the chemistry of the surfaces and surface morphologies.<sup>20</sup> Chemically modified surfaces with quaternary ammonium salts prevent the conditioning layers’ formation before bacterial deposition.<sup>40</sup> Similarly, zwitterionic surfaces and nanosilver-modified surfaces are highly effective in inhibiting bacterial attachment to surfaces.<sup>41</sup> The use of thermo-responsive



coatings showed impressive results in the prevention of bacterial attachment onto surfaces. This strategy is based on changing the nature of the surface based on the temperature of the medium by coating the surface with thermo-responsive materials, e.g., poly(*N*-isopropyl acrylamide). At high temperatures, the surface becomes hydrophobic and enables bacterial attachment, while decreasing the temperature turned the surface into a hydrophilic surface which leads to detachment of the adsorbed bacterial microcolonies.

Schiff bases are studied widely due to their synthetic flexibility, selectivity, and sensitivity toward the central metal atom, structural similarities with natural biological compounds, and also the presence of an azomethine group ( $-\text{N}=\text{CH}-$ ).<sup>42</sup> The azomethine group is considered to be the fundamental characteristic of Schiff bases which has interesting biological significance and is found to be responsible for biological activities such as fungicidal and bactericidal activities.<sup>43</sup> Another key point to remember is that Schiff bases with oxygen, nitrogen, and carbonyl groups have been used as drugs and reported to possess biological activities against bacteria and fungi due to their biochemical, clinical, and pharmacological properties.<sup>44</sup> The biological activity of Schiff bases mainly depends on the azomethine group; hence, the nitrogen atom may be involved in the formation of a hydrogen bond with the active centers of cell constituents and interferes in normal cell processes. A literature survey shows that Schiff bases show bacteriostatic and bactericidal activities.<sup>45</sup> Antibacterial, antifungal, antitumor, and anticancer activities have been reported, and they are also active against a wide range of organisms, e.g., *C. albicans*, *E. coli*, *S. aureus*, *B. polymyxa*, *P. viticola*, etc.<sup>46</sup> Throughout this work, we planned to synthesize novel dicationic surfactants (4-(4-hydroxy-3-methoxybenzylidene amino)-1-(3-(4-(4-hydroxy-3-methoxybenzylideneamino)-2,3-dihydro-5-methyl-3-oxo-2-phenyl-1H-pyrazol-2-yl)hexyl, octyl, dodecyl)-1-bromo-1,2-dihydro-3-methyl-1-phenylpyrazole-5-one (Q1–3)) to be used as biocides for resisting the growth of different bacterial biofilms. The work describes the synthesis and evaluation of the biological activities as cytotoxicity and antimicrobial properties of a series of diquaternary cationic biocides that were studied during the inhibition of microbial biofilms. The prepared compounds were synthesized by coupling reaction between vanillin and 4-aminoantipyrene to obtain a Schiff base of 4-aminoantipyrene (SB) followed by quaternization reaction using three dibromoalkanes, namely, 1,6-bromohexane, 1,8-bromooctane, and 1,12-bromododecane to obtain three diquaternary compounds Q1–3. The structure of the prepared dicationic surfactants was confirmed using elemental analyses, Fourier transform infrared spectroscopy (FTIR), and proton nuclear magnetic resonance (<sup>1</sup>H NMR) spectroscopy; antibacterial assessment and antimicrobial activity were examined by measuring the diameter of the inhibition zone. The inhibitory effects of the prepared dicationic surfactants were increased by increasing their spacer chains, and the highest inhibitory zone diameter was achieved for the Q3 biocide. The future study aims to study the effect of metal complexes and their nanofoms of the prepared diquaternary compounds on their biocidal activities against different bacterial strains.

## 2. EXPERIMENTAL SECTION

**2.1. Synthesis of Schiff Bases.** The coupling reaction has occurred between vanillin and 4-aminoantipyrene in an equimolar ratio (0.1 mole) of the two reactants in a one-

neck flask connected by a Dean–Stark connection, using xylene (100 mL) as a solvent and 0.1 wt % of dehydrating agent (*p*-toluene sulfonic acid). The reaction medium was agitated at a reflux temperature (135 °C) until 1.8 mL of H<sub>2</sub>O was obtained. Then, the product was obtained after evaporating the solvent. The product was further purified by washing with hot bidistilled water to remove the used catalyst and excess reactants, followed by drying at 70 °C under vacuum for 24 h<sup>47</sup> to obtain SB, yield = 92%.

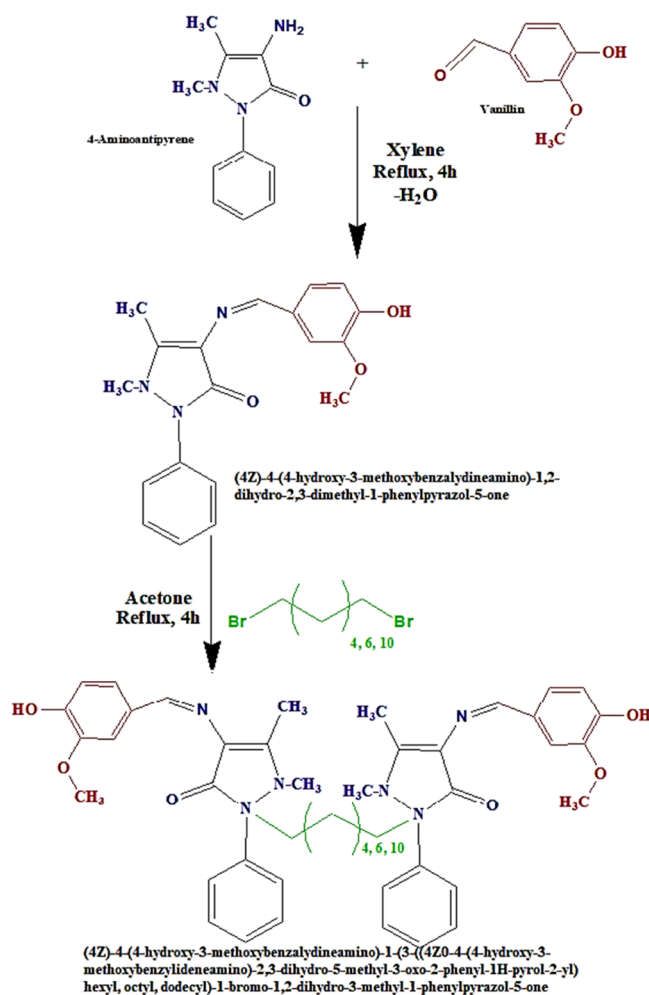
### 2.2. Synthesis of the Targeted Diquaternary Biocides.

A quaternization reaction was performed between the prepared Schiff base product (SB) and three dibromoalkanes, namely, 1,6-bromohexane, 1,8-bromooctane, and 1,12-bromododecane at a 1:2 molar ratio, respectively, in an appropriate amount of acetone as a solvent. The reaction was performed in a one-neck flask connected by a condenser, and the medium was agitated at a reflux temperature for 4 h. Then, the reaction medium was settled to precipitate the desired diquaternary products Q1–3. The obtained precipitates were filtered off, washed several times with diethyl ether, and then dried at 40 °C under vacuum for 24 h<sup>48</sup> (Scheme 1). The products were denoted as Q1–3 for the hexyl, octyl, and dodecyl derivatives, yield = 85–82, 83%.

### 2.3. Surface and Interfacial Tension Measurements.

Surface tension measurements were performed for freshly prepared Q1–3 dicationic solutions in bidistilled water in a

Scheme 1. Synthesis of Diquaternary Biocides (Q1–3)



concentration range of 0.001–10 mM at 25 °C, utilizing a Kruss-K20 tensiometer, while the interfacial tension measurements were performed between paraffin oil and surfactant solutions (0.1% concentration) at 25 °C.<sup>49</sup>

**2.4. Antimicrobial Assay.** The produced Q1–3 dicationic biocides were evaluated for antibacterial and antifungal activities toward *Staphylococcus aureus* (NCTC-7447), *E. coli* (NCTC-1041), *Bacillus subtilis* (NCIB-3610), *Pseudomonas aeruginosa* (NCIB-9016), and *Desulfomonas pigra*, popular species of sulfate-reducing bacteria (SRB). The fungistatic activity was investigated using *Aspergillus niger* (Ferm-Bam C-21) and *Candida albicans*.

The antimicrobial activities of Q1–3 dicationic biocides against fungi and bacteria were tested using the agar well diffusion technique.<sup>50</sup> The bacterial cultures were incubated in a nutrient agar medium, whereas the fungal cultures were grown in a malt medium. The bacteria were cultured in broth media for 24 h. In the case of fungi, the broth medium was cultured for 48 h before being filtered through a fine coating of antiseptic Sintered Glass G2 to eliminate mycelium particles before being utilized for inoculation.

To prepare the discs and inoculate them, 1.0 mL of inoculum was put with 50 mL of 40 °C agar medium. Agar was poured onto 120 mm Petri plates and let to cool to ambient temperature. Utilizing antiseptic tubes, wells (6 mm in diameter) were cut in the agar plates. The wells were loaded to the agar's surface with 0.1 mL of the Gemini surfactants (5 mg/mL dimethyl formamide). The plates were placed on a flat surface and incubated for 24 h at 30 °C for bacteria and 48 h for fungi before measuring the dimensions of the inhibitory zones. The inhibitory zone generated by such molecules against the bacterial strain determined the synthesized compounds' antibacterial and antifungal properties. The average score collected from three separate runs has been used to determine each sample's zone of inhibition.

**2.5. Minimum Inhibition Concentration (MIC).** The biocidal activity of the synthesized cationic surfactants (Q1–Q3) against the tested strains was expressed in terms of MIC. MIC is the minimal concentration of biocides that can inhibit the detectable growth of microorganisms after incubation for 24 h. MICs were estimated using the dilution technique. In typical procedures, the prepared biocides were dissolved in a distilled water/alcohol (3/1; v/v) mixture at different concentrations. An aliquot of the different biocide solutions, 1 mL in volume, was placed in agar media (14 mL). The final concentrations of the tested biocides were 500–6 µg/mL.

### 3. RESULTS AND DISCUSSION

**3.1. Structure Elucidation of the Prepared Compounds.** The chemical structures of the prepared Schiff base of 4-aminoantipyrene were confirmed using elemental analyses, FTIR, and <sup>1</sup>H NMR spectroscopy as follows:

(4Z)-4-(4-Hydroxy-3-methoxybenzylideneamino)-1,2-dihydro-2,3-dimethyl-1-phenyl pyrazole-5-one (SB): Yield = 92%. C,H,N = C% 68/67, H% 5.7/5.4, 13/12 N% (theo/exp). FTIR: 3100–3500 cm<sup>-1</sup> (O–H and N–H stretching),<sup>51</sup> 2862 and 2924 cm<sup>-1</sup> (asymmetric and symmetric stretching of C–H aliphatic),<sup>52,53</sup> 1658 cm<sup>-1</sup> (C=C conjugated),<sup>54,55</sup> and 1650 cm<sup>-1</sup> (–C=N-azomethine)<sup>56</sup> (Figure 3A). <sup>1</sup>H NMR: δ(ppm) = 1.72 ppm (s, 3H, CH<sub>3</sub>–C=C), 2.47 ppm (s, 3H, CH<sub>3</sub>–N), 3.7 ppm (s, 3H, CH<sub>3</sub>–O), 5.1 ppm (m, 1H, H–O–Ar), 6.68 ppm (m, 2H, mH–C–Ar), 6.71 ppm (m, 3H, o,pH–C–Ar), and 7.9 ppm (s, 1H, H–C=N-azomethine). <sup>13</sup>C NMR spectra

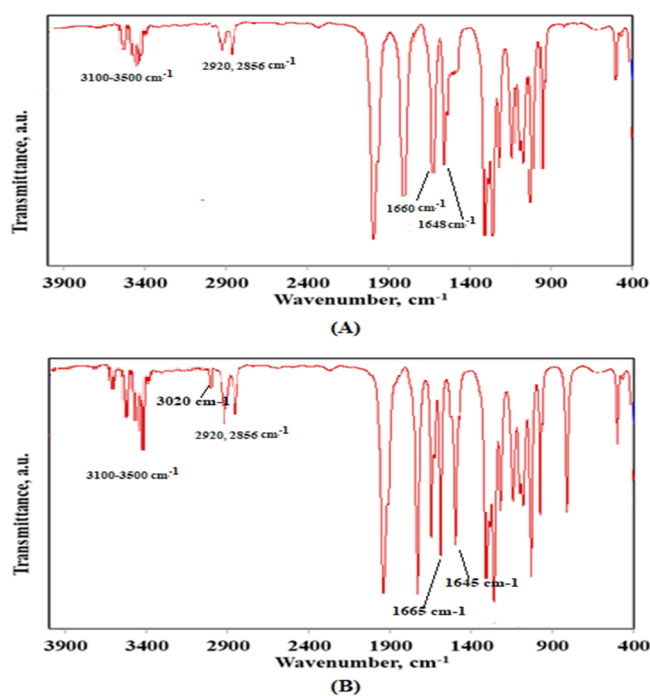


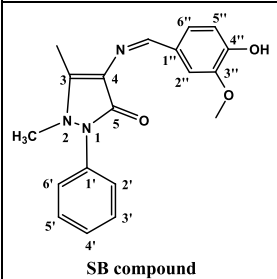
**Figure 3.** FTIR spectra of (A) 4-aminoantipyrene Schiff base (SB); (B) diquaternary biocides (Q1).

of SB showed significant distribution of the carbon atoms among the molecules,<sup>57</sup> and the chemical shifts of each signal are listed in Table 1. The formation of the new functional groups in the produced Schiff base parent compound was confirmed from the obtained FTIR, <sup>1</sup>H NMR, and <sup>13</sup>C NMR spectra.

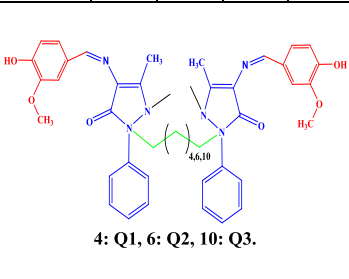
(4Z)-4-(4-Hydroxy-3-methoxybenzylideneamino)-1-(3-((4Z)-4-(4-hydroxy-3-methoxybenzylideneamino)-2,3-dihydro-5-methyl-3-oxo-2-phenyl-1H-pyrrrol-2-yl) hexyl, octyl, dodecyl)-1-bromo-1,2-dihydro-3-methyl-1-phenyl pyrazole-5-one (Q1–3): Yield = 82–85%. C,H,N (theo/exp) = Q1: 57/56 C %, 5/5 H%, 9/9 N%, and 18/18 Br%; Q2: 58/56 C%, 5/4 H%, 9/7 N%, and 17/16 Br%; Q3: 59/57 C%, 6/5 H%, 9/7 N%, and 16/14 Br%. FTIR: 3100–3500 cm<sup>-1</sup> (–OH and –NH stretching), 3025 cm<sup>-1</sup> (C–N<sup>+</sup> stretching) confirming the formation of diquaternary products, 2862 and 2932 cm<sup>-1</sup> (asymmetric and symmetric stretching of C–H aliphatic), 1668 cm<sup>-1</sup> (C=C conjugated), and 1647 cm<sup>-1</sup> (–C=N-azomethine) (Figure 3B). <sup>1</sup>H NMR: δ(ppm) = 1.73 ppm (s, 6H, CH<sub>3</sub>–C=C), 1.85 ppm (Q1: m, 8H, (–CH<sub>2</sub>–)<sub>4</sub>; Q2: m, 12H, (–CH<sub>2</sub>–)<sub>6</sub>; Q3: m, 20H, (–CH<sub>2</sub>–)<sub>10</sub>), 2.45 ppm (s, 6H, CH<sub>3</sub>–N), 3.71 ppm (s, 6H, CH<sub>3</sub>–O), 5.1 ppm (m, 2H, H–O–Ar), 6.61 ppm (m, 4H, mH–C–Ar), 6.76 ppm (m, 6H, o,pH–C–Ar), and 8.1 ppm (s, 2H, H–C=N-azomethine). <sup>13</sup>C NMR spectra of Q1–3 showed comparable chemical shifts for the carbon atoms of the parent SB compound (Table 1). After quaternization (Scheme 1), the carbon atoms of repeated methylene groups in the spacer chains showed a characteristic signal at 54.3 ppm assigned for CH<sub>2</sub>–N<sup>+</sup>, and additional signals related to the repeated carbon atoms of the hydrophobic chains (–N<sup>+</sup>–CH<sub>2</sub>–(CH<sub>2</sub>)<sub>n</sub>–CH<sub>2</sub>–N<sup>+</sup>) were assigned at 23.7–27.6 ppm for Q1; 23.7–30.3 ppm for Q2; and 23.7–30.6 ppm for Q3.<sup>58</sup> The functional groups of the produced diquaternary compounds appeared in the FTIR spectra, while the well-defined hydrogen protons were confirmed along the

**Table 1.**  $^{13}\text{C}$  NMR Shifts of the Intermediate (SB) and the Products (Q1–3)

Carbon atom	$^{13}\text{C}$ NMR chemical shifts, ppm			
	SB	Q1	Q2	Q3
CH <sub>3</sub>	13.5	13.8	13.8	13.8
N-CH <sub>3</sub>	40.5	38.2	38.2	38.2
O-CH <sub>3</sub>	57.9	57.9	57.9	57.9
C4	113.4	113.4	113.4	113.4
C2' and C6'	116.6	116.6	116.6	116.6
C2''	118.2	118.2	118.2	118.2
C5''	120.5	120.5	120.5	120.5
C4'	122.8	122.8	122.8	122.8
C6''	126.6	126.6	126.6	126.6
C1''	131.2	131.2	131.2	131.2
C3' and C5'	133.2	133.2	133.2	133.2
C1'	140.4	146.5	146.5	146.5
C4''	152.4	152.4	152.4	152.4
C3	154.7	154.7	154.7	154.7
C3''	156.0	156.0	156.0	156.0
C5	165.5	163.7	163.7	163.7
-C=N-	168.6	168.6	168.6	168.6



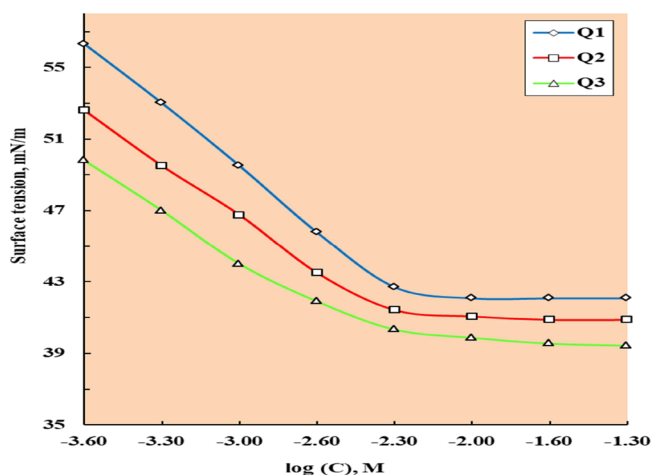
SB compound



4: Q1, 6: Q2, 10: Q3.

different diquatary compounds using  $^1\text{H}$  NMR spectroscopic analysis.

**3.2. Surface Tension ( $\gamma$ ) and Critical Micelle Concentration (CMC).** Figure 4 validates the relationship between surface tension ( $\gamma$ ) and  $-\log$  concentration (C) of the prepared diquatary biocides at 25 °C. It is noticeable that the  $\gamma$  vs  $-\log$  C relation is notable by two distinct zones. One

**Figure 4.** Surface tension-log concentration of the prepared diquatary biocides (Q1–3) at 25 °C.

is in a reduced concentration range and distinguished by a rapid decrease in surface tension values. The critical micelle concentration (CMC) is produced by the concentration at the intersection of these two locations. Furthermore, the greater reduction in surface tension values in Figure 4 demonstrates that these diquatary compounds have excellent surface activity. This is owing to the surfactant molecules' capacity to considerably reduce surface tension. Figure 4 demonstrates the importance of the lengths of Q1–3 hydrophobic chains in determining the surface tension magnitude of their solutions. This effect is caused by a greater contact between the nonpolar chains (hydrophobes) and the polar medium. To reduce that interaction, the molecules are guided toward the air–water contact, which significantly reduces surface tension. As seen in Figure 4, the length of the hydrophobic chain has a major influence on CMC values within a similar homologous chain. As the hydrophobic chain length rises, the CMC values of Q1–3 derivatives decrease. This result was described in some reported studies.<sup>59,60</sup> The CMC value of the dodecyl derivative is the lowest (Q3).

The efficiency of the surfactant compounds ( $\pi_{\text{cmc}}$ ) is described as the variation in surface tension between the surfactant solution at the CMC and the surface tension of bidistilled water at a fixed temperature according to eq 2:

$$\pi_{\text{cmc}} = \gamma_0 - \gamma_{\text{cmc}} \quad (2)$$

where  $\gamma_0$  and  $\gamma_{\text{cmc}}$  are the surface tensions of the bidistilled water and the surfactant solution at their CMC, respectively.

The efficiency values ( $\pi_{\text{cmc}}$ ) of the prepared diquatary surfactants showed high surface activity. The  $\pi_{\text{cmc}}$  value also showed improved surface activity compared to those of quaternary homologs with identical hydrophobic tails.<sup>61</sup> This impact might be attributed to the distinctive adsorption properties of these compounds at the interfaces. The hydrophobic spacer tails promote their adsorption at the interfaces that extremely lower the surface tension and increase efficacy.

However, the effectiveness ( $pC_{20}$ ) is described as the concentration of surfactant which can reduce 20 mN/m from the surface tension of bidistilled water at a given temperature and taken from the surface tension profile as the concentration related to 51.2 mN/m. It appears that effectual amphiphiles have lesser  $\pi_{\text{cmc}}$  values. The  $\pi_{\text{cmc}}$  values of Q1–3 surfactants displayed relatively low values ranging from 0.525 to 0.416 mM compared with the quaternary surfactants with identical hydrophobic tails.<sup>62</sup> The values of  $\pi_{\text{cmc}}$  and  $pC_{20}$  of the prepared surfactants (Q1–3) illustrated their potential as effectual interfacial agents in numerous uses that required great depression in the surface tension (Table 1). These results were illustrated in several reports.<sup>63,64</sup> These uses involve phase transfer catalysis, nucleic acid solubilization, gene extraction, food additives, pharmaceuticals, household products, and antimicrobial substances.

The maximum surface excess ( $\Gamma_{\text{max}}$ ) is described as the surfactant concentration at the saturation of the surface interface near the CMC.  $\Gamma_{\text{max}}$  is a good predictor of the efficacy of surfactant adsorption at the water–air interface.  $\Gamma_{\text{max}}$  of the prepared surfactants was estimated utilizing the Gibbs equation (eq 3), Table 1:

$$\Gamma_{\text{max}} = [\partial\gamma/\partial\log C]/[3 \times 2.303RT] \quad (3)$$



**Table 2. Critical Micelle Concentration (CMC), Effectiveness ( $\pi_{\text{cmc}}$ ), Efficiency ( $\text{PC}_{20}$ ), Maximum Surface Excess ( $\Gamma_{\text{max}}$ ), Minimum Surface Area ( $A_{\text{min}}$ ), and Free Energy Changes of Adsorption ( $\Delta G_{\text{ads}}$ ) and Micellization ( $\Delta G_{\text{mic}}$ ) of Q1–3 Surfactants at 25 °C**

compound	CMC, M/L	$\pi_{\text{cmc}}$ , mN/m	$\text{PC}_{20}$ , M/L	$\Gamma_{\text{max}}$ , mol/cm <sup>2</sup> × 10 <sup>-8</sup>	$A_{\text{min}}$ , nm <sup>2</sup>	$\Delta G_{\text{ads}}$ , kJ/mole	$\Delta G_{\text{mic}}$ , kJ/mole
Q1	0.000525	36	0.0000050	7.87	2.11	-22.94	-18.86
Q2	0.000495	34	0.0000071	8.21	2.02	-23.31	-19.29
Q3	0.000416	33	0.0000089	8.33	1.99	-24.18	-20.11

**Table 3. Bactericidal Activity of the Synthesized Q1–3 Biocides**

derivative	inhibition zone diameter, mm				
	<i>E. coli</i>	<i>Salmonella typhi</i>	<i>Staphylococcus aur.</i>	<i>Bacillus sub.</i>	<i>Deulfomonus pigra</i>
Q1	13.0	14.0	15.0	16.7	12.6
Q2	16.8	18.2	17.0	22.5	14.8
Q3	17.5	22.0	23.2	27.8	15.3
CTMABr	12.3	12.3	12.3	12.3	11.0

where  $R$  (universal gas constant) =  $8.31 \times 10^7$  erg/mol·K,  $T$  is the absolute temperature, and  $(\partial\gamma/\partial\log C)$  is the slope of the  $\gamma$  vs  $-\log C$  plot at ambient temperature.

However,  $A_{\text{min}}$  (the minimum surface area) is the area occupied per molecule of surfactant at the water–air interface and was estimated from the following equation (eq 4):

$$A_{\text{min}} = \frac{1}{N_A \cdot \Gamma_{\text{max}}} \quad (4)$$

where  $N_A$  is a constant and referred to several Avogadro.

The chemical composition of the hydrophobic molecules influences the values of  $\Gamma_{\text{max}}$ . Larger hydrophobes provide high surface pressure ( $\partial\gamma/\partial\log C$ ), which relates to increased surfactant molecule concentration at the interface. The increased surface concentration is because of the hydrophobe–water interface (repulsion forces) that improved due to the value reduction in hydrophobic–hydrophilic balance (HLB), which raised the surfactant molecules at the interface and therefore increased  $\Gamma_{\text{max}}$  as seen in Table 1. Raising the surface concentration (surface pressure,  $\partial\gamma/\partial\log C$ ) leads to improving the number of surfactant molecules at the interface, causing crowding and decreasing the accessible area at the interface for each molecule. The results in Table 1 show that extending the length of the hydrophobic molecules reduces the accessible area for surfactant compounds at the interface ( $A_{\text{min}}$ ).

**3.3. Standard Free Energy of Adsorption and Micellization ( $\Delta G_{\text{ads}}$  and  $\Delta G_{\text{mic}}$ ).** The chemical composition of the surfactant molecules is distinguished by the occurrence of a charged head group (one, two, or more) and lengthy alkyl chains. This is known as an amphipathic structure. This combination gives the molecule certain unique properties. These include the capacity to be present in the bulk of the solution (during micelle creation) and the ability to soak up at the air/water interface to create an organized monolayer. As a result, it is hypothesized that these two processes of adsorption and micellization happened concurrently. The predominance of the two processes is determined by variations in free energy. As a result, the free energies of adsorption ( $\Delta G_{\text{ads}}$ ) and micellization ( $\Delta G_{\text{mic}}$ ) were estimated using Rosen's approach (eqs 5 and 6).<sup>61</sup>

$$\Delta G_{\text{mic}} = -RT \ln (\text{CMC}) \quad (5)$$

$$\Delta G_{\text{ads}} = \Delta G_{\text{mic}} - (6.023 \times 10^{-1} \pi_{\text{cmc}} \cdot A_{\text{min}}) \quad (6)$$

where  $R = 8.31 \times 10^7$  erg/mol·K,  $T$  is the absolute temperature,  $\pi_{\text{cmc}}$  is the efficiency, and  $A_{\text{min}}$  is the lowest surface area.

The minus value of  $\Delta G_{\text{ads}}$  and  $\Delta G_{\text{mic}}$  (Table 2) suggests that both micellization and adsorption processes occur spontaneously at 25 °C. Comparison between  $\Delta G_{\text{ads}}$  and  $\Delta G_{\text{mic}}$  values of the prepared surfactants showed the greater negative values of  $\Delta G_{\text{ads}}$  suggesting the amphiphiles' proclivity for adsorption. However, at the same time, they exhibit a good tendency toward micellization.

**3.4. Cytotoxic Activity of Prepared Cationic Gemini Surfactants.** The bacterial cell membrane is thought to be made up of phospholipids and particular amino acids. The cellular membrane's functioning is primarily the dissemination of the constituents required for biological processes and the excretion of the wastes created.<sup>65</sup> The selective permeability determines the regulation of the two processes. The charged amino acids (teichoic acid derivatives) in the outer cellular membrane govern the entry or exit of the polar species into or out of the cells, whereas phospholipids and peptidoglycans play this role for nonpolar materials.<sup>66</sup> When the preferential permeability of the cell membranes damages the vital biological processes, death of the microorganisms occurs. Bacterial and fungal biocides achieved their lethal role on the microorganisms by breaking and/or destroying the high selectivity of the cellular membranes. This behavior commonly occurs in the case of cationic biocides. The antibacterial and antifungal effectiveness was determined by the inhibition zone diameter method of the produced dicationic biocides against several microorganisms (*E. coli*, *Staphylococcus aureus*, *Pseudomonas aeruginosa*, *Bacillus subtilis*, and *Desulfomonas pigra*), which was high as depicted in Table 3. The inhibitory effects of Q1–3 were increased by increasing their spacer chain length, and the highest inhibitory zone diameter was obtained for the Q3 biocide against *E. coli*, *Salmonella typhi*, *Staphylococcus aureus*, and *Pseudomonas aeruginosa* at 17.5, 22.0, 23.2, and 27.8 mm, referring to the used reference (cetyl trimethyl ammonium bromide, CTABr, 12.3 mm), respectively. These results were in comparison with the reported results of SRB using cationic biocides.<sup>43,50</sup>

Several variables including structural and interfacial characteristics contribute to the excellent antibacterial activity of cationic surfactants. The benzene ring nucleus, the aliphatic hydrocarbon chains, azomethine groups, and positively charged head groups ( $\text{N}^+$ ) are all structural elements. Low

effectiveness, efficiency, low surface area, and high surface concentration are examples of interfacial factors.<sup>67</sup> The existence of aliphatic chains promotes the adsorption of the cationic biocides onto the cellular membranes of the microorganisms because of the matching behavior between the aliphatic chains of their molecules and the nonpolar chains which constituted the bacterial lipid layers. The existence of positive charges at the biocide molecules (Q1–3) is attached to the negatively charged teichoic acid derivatives that participated in the cellular membranes. Furthermore, the highly interfacial activities of the biocides facilitate the contact between the external components and the cellular membrane while suppressing the selective permeability. As a result, the microorganisms' biochemical reactions and metabolic pathways are affected, resulting in the death of microorganisms.<sup>68</sup> Q3 displayed the highest efficiency against the tested bacterial strains. This was ascribed to its greater efficacy values as well as a higher maximum surface excess. Higher efficiency values suggest a proclivity for adsorption at various surfaces, including bacterial membranes. Furthermore, the improved surface excess demonstrated the presence of the adsorbed Q3 molecules at high concentrations at the interfaces. The antibacterial properties of Q1–3 biocides were shown to be effective against SRB (*Deulfomonus pigra*). However, these values are still lower than those of the other examined bacterial strains, as shown in Table 2. This might be attributed to the SRB strain's resistance to harsh factors in the environment due to the stiffness of their cell membranes.

The antifungal behaviors of Q1–3 biocides against *Candida albicans* and *Aspergillus niger* are illustrated in Table 4. The

**Table 4. Fungicidal Activity of the Synthesized Q1–3 Biocides**

derivative	inhibition zone diameter, mm *	
	<i>Aspergillus niger</i>	<i>Aspergillus flavus</i>
Q1	15.7	16.3
Q2	19.2	18.2
Q3	24.5	25.4
Grisofulvine	11.6	11.6

recorded inhibition zones ranged between 15.7 and 25.4 mm, referring to the used reference (Grisofulvine, 11.6 mm), indicating their high cytotoxic activities toward the examined fungus. The inhibition diameter values revealed that cytotoxic efficacies of Q1–3 are significantly associated with their interfacial characteristics, mainly their efficacy and maximum surface excess. The cytotoxic efficiencies of Q1–3 biocides were demonstrated to have an excellent inhibitory propensity against various bacterial species and fungi. The potencies of

these biocides can be referred to as the presence of azomethine groups ( $-N=C-$ ) and diquaternary ( $-N^+-N^+-$ ) groups in these molecules. The existence of these groups promotes the adsorption of the molecule at the microorganism's outer membranes, while the existence of bromide ions (counter ions) allows them to pass readily across these membranes. As a result, the biological response in the cells is severely harmed, which leads to cell mortality.

**3.5. Minimum Inhibitory Concentration (MIC).** MICs of the prepared biocides Q1–Q3 and cetyl trimethyl ammonium bromide (CTMABr) are listed in Table 5. MIC values of CTABr ranged between 20 and 600  $\mu\text{M}$ . Comparison of the results of MICs of the tested compounds and the reference biocide (CTABr) revealed their higher efficacies compared to CTMABr for combat SRB in oil and gas reservoir protection applications; the use of cationic surfactants with low antimicrobial activity would be necessary because they present high biodegradability and less toxicity.<sup>69</sup> The results of the MIC study showed that the increase in the space chain length of the prepared biocides increased their efficiencies toward the different types of bacterial cells. Q1 showed the lowest efficiency toward the bacterial strains in a concentration range of 50–200  $\mu\text{M}$ , while Q3 performed the maximum efficiency with the lower concentration ranges of 6–20  $\mu\text{M}$ . The mode of action of the cationic biocides upon the different germs is generally preceded via an adsorption mechanism. In this mechanism, the biocides adsorb onto the negative centers on the cellular membranes. The adsorption leads to deducing cellular osmotic stability and outflow of biological constituents in the cells.<sup>70</sup> Several proposed mechanisms can explain the action mode of the biocides on the microorganisms based on the type of the bacterial strain (gram +ve or gram -ve) including impermeable coat formation on the bacterial membranes, penetration of smaller biocide molecules into the cells, and their interaction by the oppositely charged sites in the cell, and inhibition of bacterial growth through chelation of trace metals.<sup>71,72</sup>

It is clear that *P. aeruginosa* and *S. typhimurium* species exhibited higher resistivity toward the prepared biocides and also against the used reference. This can be attributed to the nature of the chemical composition of their cellular membranes. It is reported that gram-negative bacteria are more resistant to several types of biocides than gram-positive bacteria, due to the types of constituents in the cellular membranes of each type.<sup>73</sup> The lipopolysaccharides and proteins in the gram-negative bacterial cell membrane limit the biocide molecules' penetration into the bacterial cells. Consequently, their diffusion into these types of cells required sufficient acceptability between the HLB of the biocide molecules and the cellular membrane constituents. The

**Table 5. Minimum Inhibitory Concentration Values, MIC<sup>a</sup> ( $\mu\text{M}$ ) of the Synthesized Biocides Q1–3 against Different Bacterial Strains**

biocides	bacteria					
	<i>S. aureus</i> ATCC 29213	<i>B. subtilis</i> ATCC 55422	<i>E. coli</i> ATCC 25922	<i>P. aeruginosa</i> ATCC 27853	<i>S. typhimurium</i> ATCC 27948	<i>Desulfomonas pigra</i> ATCC 29098
Q1	50	50	200	600	>600	200
Q2	50	20	100	500	>600	100
Q3	20	6	20	400	>600	50
CTMABr	20	50	100	300	600	400

<sup>a</sup>The data are a mean of five replicates with relative error ~7%.



prepared cationic biocides were monitored for their toxicity toward SRB (*D. pigra*) (Table 5). The data showed promising results due to their comparatively higher efficacies against SRB. SRB (anaerobic bacteria) released H<sub>2</sub>S gas in oilfields due to their ability to reduce sulfur-containing compounds in crude oil. The MIC values of the prepared cationic biocides showed acceptable efficacies against SRB. It is clear (Table 5) that the gradual increase of the hydrophobic chain length of the synthesized surfactants increases their biocidal activities against SRB.

The prepared Schiff base and the corresponding quaternary derivatives showed noticeable antibacterial and antifungal activities against various lethal microorganisms. Additionally, these biocides showed efficiency in the petroleum industry regarding the prevention of SRB growth to prevent the production of the most hazardous gas, hydrogen sulfide. The essential positive impact of the prepared compounds on the environment is mainly the prevention of H<sub>2</sub>S formation in oilfields.

#### 4. CONCLUSIONS

The chemical structures of the diquaternary cationic surfactants showed a high influence on their surface activities. The CMC, effectiveness, and maximum surface excess values were decreased by increasing the alkyl chain spacers, while the minimum surface area was increased. Inhibition zone diameter evaluation showed increased inhibition area by increasing the surface activity of the synthesized biocides. Q3 showed the highest area of inhibition against the tested bacterial strains. The growth of SRB was highly inhibited by applying the prepared biocides compared to the traditional biocides. The prepared biocides Q1–Q3 showed promising results due to their comparatively higher efficacies against SRB. The MIC values of the prepared cationic biocides presented acceptable efficacies against SRB. The essential positive impact of the prepared compounds on the environment is mainly the prevention of H<sub>2</sub>S formation in oilfields.

#### AUTHOR INFORMATION

##### Corresponding Authors

Nabel A. Negm – Egyptian Petroleum Research Institute, Cairo EG 11776, Egypt; Email: [nabelnegm@hotmail.com](mailto:nabelnegm@hotmail.com)

Eslam A. Mohamed – Egyptian Petroleum Research Institute, Cairo EG 11776, Egypt; [orcid.org/0000-0002-5787-5882](https://orcid.org/0000-0002-5787-5882); Email: [eslamazmy60@yahoo.com](mailto:eslamazmy60@yahoo.com)

##### Authors

Amal A. Altalhi – Department of Chemistry, College of Science, Taif University, Taif 21944, Saudi Arabia

Nermin E. Saleh Mohamed – Egyptian Petroleum Research Institute, Cairo EG 11776, Egypt

Maram T. H. A. Kana – National Institute of LASER Enhanced Science, Cairo University, Giza 11776, Egypt

Complete contact information is available at:

<https://pubs.acs.org/10.1021/acsomega.2c04836>

##### Notes

The authors declare no competing financial interest.

#### ACKNOWLEDGMENTS

The authors would like to acknowledge Taif University Researcher supporting project number (TURP-2020/243),

Taif University, Taif, Saudi Arabia. Also, the authors would like to thank Egyptian Petroleum Research Institute (EPRI).

#### REFERENCES

- (1) Bedoya, K.; Niño, J.; Acero, J.; Cabarcas, F.; Alzate, J. F. Assessment of the Microbial Community and Biocide Resistance Profile in Production and Injection Waters from an Andean Oil Reservoir in Colombia. *Int. Biodeterior. Biodegrad.* **2021**, *157*, No. 105137.
- (2) Zhao, J.-Y.; Hu, B.; Dolfing, J.; Li, Y.; Tang, Y.-Q.; Jiang, Y.; Chi, C.-Q.; Xing, J.; Nie, Y.; Wu, X.-L. Thermodynamically Favorable Reactions Shape the Archaeal Community Affecting Bacterial Community Assembly in Oil Reservoirs. *Sci. Total Environ.* **2021**, *781*, No. 146506.
- (3) Khan, M. A. A.; Hussain, M.; Djavanroodi, F. Microbiologically Influenced Corrosion in Oil and Gas Industries: A Review. *Int. J. Corros. Scale Inhib.* **2021**, *10*, 80–106.
- (4) El-Gendy, N. S.; Hamdy, A.; Fatthallah, N. A.; Omran, B. A. Recycling of Some Domestic Wastes to Produce Green Corrosion Inhibitors and Biocides for Sulfate Reducing Bacteria. *Energy Sources, Part A* **2016**, *38*, 3722–3732.
- (5) Balakrishnan, A.; Rajasekar, A.; Venkatachari, G.; Maruthamuthu, S. Effect of Thermophilic Sulphate-Reducing Bacteria (*Desulfotomaculum Geothermicum*) Isolated from Indian Petroleum Refinery on the Corrosion of Mild Steel. *Curr. Sci.* **2009**, *97*, 342.
- (6) Daly, S.; Casey, E.; Semião, A. J. C. Osmotic Backwashing of Forward Osmosis Membranes to Detach Adhered Bacteria and Mitigate Biofouling. *J. Membr. Sci.* **2021**, *620*, No. 118838.
- (7) Parreira, P.; Martins, M. C. L. The Biophysics of Bacterial Infections: Adhesion Events in the Light of Force Spectroscopy. *Cell Surf.* **2021**, *7*, No. 100048.
- (8) Yang, Z.; Wang, J.; Shang, C.; Yang, S.; Hao, Y.; Tang, X.; Xiao, H. Spatial and Temporal Changes in Bacterial Community Structure in Adjacent Waters of Dagu River Estuary of Jiaozhou Bay (China) Revealed by High-Throughput Sequencing. *Reg. Stud. Mar. Sci.* **2022**, *52*, No. 102302.
- (9) Lee, M. M. S.; Wu, Q.; Chau, J. H. C.; Xu, W.; Yu, E. Y.; Kwok, R. T. K.; Lam, J. W. Y.; Wang, D.; Tang, B. Z. Leveraging Bacterial Survival Mechanism for Targeting and Photodynamic Inactivation of Bacterial Biofilms with Red Natural AlEgen. *Cell Rep. Phys. Sci.* **2022**, *3*, No. 100803.
- (10) Kokilaramani, S.; Narenkumar, J.; AlSalhi, M. S.; Devanesan, S.; Obulisamy, P. K.; Balagurunathan, R.; Rajasekar, A. Evaluation of Crude Methanolic Mangrove Leaves Extract for Antibiofilm Efficacy against Biofilm-Forming Bacteria on a Cooling Tower Wastewater System. *Arab. J. Chem.* **2022**, *15*, No. 103948.
- (11) Mirzaei, R.; Ranjbar, R. Hijacking Host Components for Bacterial Biofilm Formation: An Advanced Mechanism. *Int. Immunopharmacol.* **2022**, *103*, No. 108471.
- (12) Hansen, M. F.; Lo Svenningsen, S.; Røder, H. L.; Middelboe, M.; Burmølle, M. Big Impact of the Tiny: Bacteriophage–Bacteria Interactions in Biofilms. *Trends Microbiol.* **2019**, *27*, 739–752.
- (13) Kokilaramani, S.; Al-Ansari, M. M.; Rajasekar, A.; Al-Khattaf, F. S.; Hussain, A.; Govarthanan, M. Microbial Influenced Corrosion of Processing Industry by Re-Circulating Waste Water and Its Control Measures - A Review. *Chemosphere* **2021**, *265*, No. 129075.
- (14) Ghosh, S.; Sarkar, T.; Chakraborty, R. Formation and Development of Biofilm- an Alarming Concern in Food Safety Perspectives. *Biocatal. Agric. Biotechnol.* **2021**, *38*, No. 102210.
- (15) Lee, S. W.; Phillips, K. S.; Gu, H.; Kazemzadeh-Narbat, M.; Ren, D. How Microbes Read the Map: Effects of Implant Topography on Bacterial Adhesion and Biofilm Formation. *Biomaterials* **2021**, *268*, No. 120595.
- (16) Even, C.; Marlière, C.; Ghigo, J.-M.; Allain, J.-M.; Marcellan, A.; Raspaud, E. Recent Advances in Studying Single Bacteria and Biofilm Mechanics. *Adv. Colloid Interface Sci.* **2017**, *247*, 573–588.
- (17) Narenkumar, J.; Devanesan, S.; AlSalhi, M. S.; Kokilaramani, S.; Ting, Y.-P.; Rahman, P. K. S. M.; Rajasekar, A. Biofilm Formation on

Copper and Its Control by Inhibitor/Biocide in Cooling Water Environment. *Saudi J. Biol. Sci.* **2021**, *28*, 7588–7594.

(18) Chi, Y.; Huang, Y.; Wang, J.; Chen, X.; Chu, S.; Hayat, K.; Xu, Z.; Xu, H.; Zhou, P.; Zhang, D. Two Plant Growth Promoting Bacterial *Bacillus* Strains Possess Different Mechanisms in Adsorption and Resistance to Cadmium. *Sci. Total Environ.* **2020**, *741*, No. 140422.

(19) Chang, E.; Brewer, A. W.; Park, D. M.; Jiao, Y.; Lammers, L. N. Surface Complexation Model of Rare Earth Element Adsorption onto Bacterial Surfaces with Lanthanide Binding Tags. *Appl. Geochem.* **2020**, *112*, No. 104478.

(20) Uneputty, A.; Dávila-Lezama, A.; Garibo, D.; Oknianska, A.; Bogdanchikova, N.; Hernández-Sánchez, J. F.; Susarrey-Arce, A. Strategies Applied to Modify Structured and Smooth Surfaces: A Step Closer to Reduce Bacterial Adhesion and Biofilm Formation. *Colloid Interface Sci. Commun.* **2022**, *46*, No. 100560.

(21) Le Quémener, E. D.; Bouchez, T. A Thermodynamic Theory of Microbial Growth. *ISME J.* **2014**, *8*, 1747–1751.

(22) Dąbrowski, A. Adsorption – From Theory to Practice. *Adv. Colloid Interface Sci.* **2001**, *93*, 135–224.

(23) Oh, J. K.; Yegin, Y.; Yang, F.; Zhang, M.; Li, J.; Huang, S.; Verkhoturourov, S. V.; Schweikert, E. A.; Perez-Lewis, K.; Scholar, E. A.; Taylor, T. M.; Castillo, A.; Cisneros-Zevallos, L.; Min, Y.; Akbulut, M. The Influence of Surface Chemistry on the Kinetics and Thermodynamics of Bacterial Adhesion. *Sci. Rep.* **2018**, *8*, 17247.

(24) Demirdjian, S.; Schutz, K.; Wargo, M. J.; Lam, J. S.; Berwin, B. The Effect of Loss of O-Antigen Ligase on Phagocytic Susceptibility of Motile and Non-Motile *Pseudomonas Aeruginosa*. *Mol. Immunol.* **2017**, *92*, 106–115.

(25) Haiko, J.; Westerlund-Wikström, B. The Role of the Bacterial Flagellum in Adhesion and Virulence. *Biology* **2013**, *2*, 1242–1267.

(26) Zhang, Y.; Liu, H.; Gu, D.; Lu, X.; Zhou, X.; Xia, X. Transcriptomic Analysis of PhoR Reveals Its Role in Regulation of Swarming Motility and T3SS Expression in *Vibrio Parahaemolyticus*. *Microbiol. Res.* **2020**, *235*, No. 126448.

(27) Cheng, Y.; Moraru, C. I. Long-Range Interactions Keep Bacterial Cells from Liquid-Solid Interfaces: Evidence of a Bacteria Exclusion Zone near Nafion Surfaces and Possible Implications for Bacterial Attachment. *Colloids Surf., B* **2018**, *162*, 16–24.

(28) Santana, H. J. A.; Caseli, L. A Bactericide Peptide Changing the Static and Dilatational Surface Elasticity Properties of Zwitterionic Lipids at the Air-Water Interface: Relationship with the Thermodynamic, Structural and Morphological Properties. *Biophys. Chem.* **2021**, *277*, No. 106638.

(29) Zhang, X.; Wu, Y.; Li, Y.; Li, B.; Pei, Y.; Liu, S. Effects of the Interaction between Bacterial Cellulose and Soy Protein Isolate on the Oil-Water Interface on the Digestion of the Pickering Emulsions. *Food Hydrocolloids* **2022**, *126*, No. 107480.

(30) Al-Wrafy, F. A.; Al-Gheethi, A. A.; Ponnusamy, S. K.; Noman, E. A.; Fattah, S. A. Nanoparticles Approach to Eradicate Bacterial Biofilm-Related Infections: A Critical Review. *Chemosphere* **2022**, *288*, No. 132603.

(31) Park, S.; Sauer, K. SagS and Its Unorthodox Contributions to *Pseudomonas Aeruginosa* Biofilm Development. *Biofilm* **2021**, *3*, No. 100059.

(32) Chao, Y.; Zhang, T. Probing Roles of Lipopolysaccharide, Type 1 Fimbria, and Colanic Acid in the Attachment of *Escherichia Coli* Strains on Inert Surfaces. *Langmuir* **2011**, *27*, 11545–11553.

(33) Eom, G. T.; Oh, J. Y.; Park, J. H.; Lim, H. J.; Lee, S. J.; Kim, E. Y.; Choi, J.-E.; Jegal, J.; Song, B. K.; Yu, J.-H.; Song, J. K. Alleviation of Temperature-Sensitive Secretion Defect of *Pseudomonas Fluorescens* ATP-Binding Cassette (ABC) Transporter, TliDEF, by a Change of Single Amino Acid in the ABC Protein, TliD. *J. Biosci. Bioeng.* **2016**, *122*, 283–286.

(34) Kreve, S.; Reis, A. C. D. Bacterial Adhesion to Biomaterials: What Regulates This Attachment? A Review. *Jpn. Dent. Sci. Rev.* **2021**, *57*, 85–96.

(35) Bouckaert, J.; Mackenzie, J.; de Paz, J. L.; Chipwaza, B.; Choudhury, D.; Zavialov, A.; Mannerstedt, K.; Anderson, J.; Piérard,

D.; Wyns, L.; Seeberger, P. H.; Oscarson, S.; De Greve, H.; Knight, S. D. The Affinity of the FimH Fimbrial Adhesin Is Receptor-Driven and Quasi-Independent of *Escherichia Coli* Pathotypes. *Mol. Microbiol.* **2006**, *61*, 1556–1568.

(36) Nilsson, L. M.; Thomas, W. E.; Trintchina, E.; Vogel, V.; Sokurenko, E. V. Catch Bond-Mediated Adhesion without a Shear Threshold: Trimannose versus Monomannose Interactions with the FimH Adhesin of *Escherichia Coli*. *J. Biol. Chem.* **2006**, *281*, 16656–16663.

(37) Marina, C.; Cristina, B.; Eleonora, S.; Roberto, R. Environmental, Microbiological, and Immunological Features of Bacterial Biofilms Associated with Implanted Medical Devices. *Clin. Microbiol. Rev.* **2022**, *35*, No. e0022120.

(38) Doiron, K.; Beaulieu, L.; St-Louis, R.; Lemarchand, K. Reduction of Bacterial Biofilm Formation Using Marine Natural Antimicrobial Peptides. *Colloids Surf., B* **2018**, *167*, 524–530.

(39) Ebnesajjad, S.; Grot, W. Fluorinated Ionomers: History, Properties, and Applications. In *Plastics Design Library*; Ebnesajjad, S. B. T.-L., second ed.; William Andrew Publishing: Oxford, 2021; pp 369–378.

(40) Hora, P. I.; Pati, S. G.; McNamara, P. J.; Arnold, W. A. Increased Use of Quaternary Ammonium Compounds during the SARS-CoV-2 Pandemic and Beyond: Consideration of Environmental Implications. *Environ. Sci. Technol. Lett.* **2020**, *7*, 622.

(41) Adlhart, C.; Verran, J.; Azevedo, N. F.; Olmez, H.; Keinänen-Toivola, M. M.; Gouveia, I.; Melo, L. F.; Crijns, F. Surface Modifications for Antimicrobial Effects in the Healthcare Setting: A Critical Overview. *J. Hosp. Infect.* **2018**, *99*, 239–249.

(42) Negm, N. A.; Zaki, M. F.; Salem, M. A. I. Cationic Schiff Base Amphiphiles and Their Metal Complexes: Surface and Biocidal Activities against Bacteria and Fungi. *Colloids Surf., B* **2010**, *77*, 96–103.

(43) Negm, N. A.; El-Farragy, A. F.; Mohammad, I. A. Synthesis and Inhibitory Activity of Schiff Base Surfactants Derived from Tannic Acid against Bacteria and Fungi. *Egypt. J. Chem.* **2012**, *55*, 367–379.

(44) Shaban, S. M.; Saied, A.; Tawfik, S. M.; Abd-Elal, A.; Aiad, I. Corrosion Inhibition and Biocidal Effect of Some Cationic Surfactants Based on Schiff Base. *J. Ind. Eng. Chem.* **2013**, *19*, 2004–2009.

(45) Nartop, D.; Özkan, E. H.; Gündem, M.; Çeker, S.; Açar, G.; Ögütçü, H.; Sari, N. Synthesis, Antimicrobial and Antitumorigenic Effects of Novel Polymeric-Schiff Bases Including Indol. *J. Mol. Struct.* **2019**, *1195*, 877–882.

(46) Moustafa, A. H.; Sayed, G. H.; Zakaria, K.; Negm, N. A.; et al. *J. Basic Environ. Sci.* **2020**, *7*, 13–21.

(47) Negm, N. A.; Badr, E. A.; Aiad, I. A.; Zaki, M. F.; Said, M. M. Investigation the Inhibitory Action of Novel Diquaternary Schiff Dibases on the Acid Dissolution of Carbon Steel in 1M Hydrochloric Acid Solution. *Corros. Sci.* **2012**, *65*, 77–86.

(48) Negm, N.; Hafiz, A. A.; Awady, M. Y. Influence of Structure on the Cationic Polytriethanolammonium Bromide Derivatives. I. Synthesis, Surface and Thermodynamic Properties. *Egypt. J. Chem.* **2004**, *47*, 369–381.

(49) Negm, N.; El, A.; Emam, D.; Mohamad, H. Environmentally Friendly Nonionic Surfactants Derived from Tannic Acid: Synthesis, Characterization and Surface Activity. *J. Surfactants Deterg.* **2012**, *15*, 433.

(50) Negm, N. A.; El Faragy, A. F.; Al Sabagh, A. M.; Abdelrahman, N. R.; Al-Sabagh, A.; Abdelrahman, N. R. New Schiff Base Cationic Surfactants: Surface and Thermodynamic Properties and Applicability in Bacterial Growth and Metal Corrosion Prevention. *J. Surfactants Deterg.* **2011**, *14*, 505–514.

(51) Farag, A. A.; Mohamed, E. A.; Sayed, G. H.; Anwer, K. E. Experimental/Computational Assessments of API Steel in 6 M H<sub>2</sub>SO<sub>4</sub> Medium Containing Novel Pyridine Derivatives as Corrosion Inhibitors. *J. Mol. Liq.* **2021**, *330*, No. 115705.

(52) Anwer, K. E.; Farag, A. A.; Mohamed, E. A.; Azmy, E. M.; Sayed, G. H. Corrosion Inhibition Performance and Computational Studies of Pyridine and Pyran Derivatives for API X-65 Steel in 6M H<sub>2</sub>SO<sub>4</sub>. *J. Ind. Eng. Chem.* **2021**, *97*, 523.

- (53) Negm, N. A.; Abubshait, H. A.; Abubshait, S. A.; Abou Kana, M. T. H.; Mohamed, E. A.; Betiha, M. M. Performance of Chitosan Polymer as Platform during Sensors Fabrication and Sensing Applications. *Int. J. Biol. Macromol.* **2020**, *165*, 402–435.
- (54) Abubshait, H. A.; Farag, A. A.; El-Raouf, M. A.; Negm, N. A.; Mohamed, E. A. Graphene Oxide Modified Thiosemicarbazide Nanocomposite as an Effective Eliminator for Heavy Metal Ions. *J. Mol. Liq.* **2021**, *327*, No. 114790.
- (55) Negm, N. A.; Sayed, G. H.; Yehia, F. Z.; Dimitry, O. I. H.; Rabie, A. M.; Azmy, E. A. M. Production of Biodiesel Production from Castor Oil Using Modified Montmorillonite Clay. *Egypt. J. Chem.* **2016**, *59*, 1045–1060.
- (56) Hashem, H. E.; Mohamed, E. A.; Farag, A. A.; Negm, N. A.; Azmy, E. A. M. New Heterocyclic Schiff Base-Metal Complex: Synthesis, Characterization, Density Functional Theory Study, and Antimicrobial Evaluation. *Appl. Organomet. Chem.* **2021**, *35*, No. e6322.
- (57) Sönmez, M.; Sogukomerogullari, H. G.; Öztemel, F.; Berber, I. Synthesis and Biological Evaluation of a Novel ONS Tridentate Schiff Base Bearing Pyrimidine Ring and Some Metal Complexes. *Med. Chem. Res.* **2014**, *23*, 3451–3457.
- (58) Hussain, S. M. S.; Kamal, M. S.; Solling, T.; Murtaza, M.; Fogang, L. T. Surface and Thermal Properties of Synthesized Cationic Poly(Ethylene Oxide) Gemini Surfactants: The Role of the Spacer. *RSC Adv.* **2019**, *9*, 30154–30163.
- (59) Mozrzymas, A. On the Hydrophobic Chains Effect on Critical Micelle Concentration of Cationic Gemini Surfactants Using Molecular Connectivity Indices. *Monatsh. Chem.* **2020**, *151*, 525–531.
- (60) Wang, Z.; Song, H. The Synthesis of Quaternary N-Alkyl Tropinium Cationic Surfactants and Study on Their Properties: Effect of Temperature, Hydrophobic Chain Length and Anions. *J. Mol. Struct.* **2022**, *1268*, No. 133732.
- (61) Shafek, S. H.; Abubshait, S. A.; Abubshait, H. A.; Negm, N. A. Antimicrobial Potentials and Surface Activities of Novel Di-Schiff Base Nonionic Surfactants Bearing Unsaturated Hydrophobic Tails. *J. Mol. Liq.* **2019**, *290*, No. 110986.
- (62) Negm, N. A.; Said, M. M.; Morsy, S. M. I. Pyrazole Derived Cationic Surfactants and Their Tin and Copper Complexes: Synthesis, Surface Activity, Antibacterial and Antifungal Efficacy. *J. Surfactants Deterg.* **2010**, *13*, 521–528.
- (63) Negm, N. A.; Morsy, S. M. I.; Said, M. M. Biocidal Activity of Some Mannich Base Cationic Derivatives. *Bioorg. Med. Chem.* **2005**, *13*, 5921–5926.
- (64) El-Tabei, A. S.; Hegazy, M. A.; Bedair, A. H.; El Basiony, N. M.; Sadeq, M. A. Novel Macrocyclic Cationic Surfactants: Synthesis, Experimental and Theoretical Studies of Their Corrosion Inhibition Activity for Carbon Steel and Their Antimicrobial Activities. *J. Mol. Liq.* **2022**, *345*, No. 116990.
- (65) Farag, A. A.; Eid, A. M.; Shaban, M. M.; Mohamed, E. A.; Raju, G. Integrated Modeling, Surface, Electrochemical, and Biocidal Investigations of Novel Benzothiazoles as Corrosion Inhibitors for Shale Formation Well Stimulation. *J. Mol. Liq.* **2021**, *336*, No. 116315.
- (66) Negm, N. A.; Abd-Elal, A. A.; Mohamed, D. E.; El-Farargy, A. F.; Mohamed, S. Synthesis and Evaluation of Silver Nanoparticles Loaded with Gemini Surfactants: Surface and Antimicrobial Activity. *J. Ind. Eng. Chem.* **2015**, *24*, 34–41.
- (67) Mohamed, D. E.; Negm, N. A.; Mishrif, M. R. Micellization and Interfacial Interaction Behaviors of Gemini Cationic Surfactants-CTAB Mixed Surfactant Systems. *J. Surfactants Deterg.* **2013**, *16*, 723–731.
- (68) Migahed, M. A.; Negm, N. A.; Shaban, M. M.; Ali, T. A.; Fadda, A. A. Synthesis, Characterization, Surface and Biological Activity of Diquaternary Cationic Surfactants Containing Ester Linkage. *J. Surfactants Deterg.* **2016**, *19*, 119–128.
- (69) Garcia, M. T.; Ribosa, I.; Kowalczyk, I.; Pakiet, M.; Brycki, B. Biodegradability and Aquatic Toxicity of New Cleavable Betainate Cationic Oligomeric Surfactants. *J. Hazard. Mater.* **2019**, *371*, 108–114.
- (70) Al-Adham, I.; Dinning, A.; Austin, P.; Collier, P. Cell Membrane Effects of Some Common Biocides. *J. Ind. Microbiol. Biotechnol.* **1998**, *21*, 6–10.
- (71) Jones, I. A.; Joshi, L. T. Biocide Use in the Antimicrobial Era: A Review. *Molecules* **2021**, *26*, 2276.
- (72) Zaky, M. F.; Sabbah, I. A.; Negm, N. A.; Hendawy, M. E. Biocidal Activity and Corrosion Inhibition of Some Cationic Surfactants Derived from Thiol Polyurethane. *Egypt. J. Chem.* **2017**, *61*, 45–60.
- (73) Qiu, H.; Si, Z.; Luo, Y.; Feng, P.; Wu, X.; Hou, W.; Zhu, Y.; Chan-Park, M. B.; Xu, L.; Huang, D. The Mechanisms and the Applications of Antibacterial Polymers in Surface Modification on Medical Devices. *Front. Bioeng. Biotechnol.* **2020**, *8*, 910.